

Inhomogeneous nucleation and growth of cavities in irradiated materials

S. L. Dudarev

EURATOM/UKAEA Fusion Association, Culham Science Centre, Abingdon, Oxfordshire OX14 3DB, United Kingdom

(Received 29 February 2000; revised manuscript received 17 May 2000)

The origin of the effect of inhomogeneous swelling observed near grain boundaries in irradiated materials is examined taking into account both nucleation and diffusional growth of cavities, and the interaction of cavities with mobile interstitial clusters produced in collision cascades. The model shows the formation of a characteristic profile of inhomogeneous swelling that exhibits features similar to those observed experimentally. The rate of swelling is found to be strongly dependent on the size of cavities, with cavities growing near the boundary being able to reach substantially larger sizes than those growing in the interior area of the grain. The distance z^* between the peak of swelling and the grain boundary scales with the density of cavities N_0 as $z^* \sim N_0^{-\beta}$, where β is close to 1/3.

I. INTRODUCTION

The kinetics of phase transformations in materials driven far from equilibrium has recently attracted considerable attention stimulated by the need to develop better understanding of how materials behave in a hostile environment.¹ A typical example of an evolving nonequilibrium system is given by a material irradiated by a flux of energetic particles,² and this is rapidly becoming one of the issues central to the design of a fusion power station.^{3,4}

The evolution of the microstructure of an irradiated material is characterized by the presence of dynamic quasiequilibrium between the generation of lattice defects by the incident energetic particles and the annihilation of these defects by dislocations, grain boundaries, and cavities in the material. A chemical reaction-type theory describing the temporal evolution of *spatially averaged* concentrations of vacancies and interstitial atoms in the presence of randomly distributed mesoscopic lattice defects was formulated 30 years ago by Brailsford and Bullough.⁵ Recent theoretical advances have been associated with the development of a more accurate treatment of effects of cascade damage. Effects of cascade damage are described by either the molecular dynamics,^{6,7} the kinetic Monte Carlo⁸ or the continuum⁹ models. One of the important aspects that emerges from recent theoretical studies concerns the importance of taking into account spatial fluctuations of concentrations of defects in the material, see, e.g., Refs. 10–13.

Spatially inhomogeneous concentration profiles naturally appear in the treatment of kinetics of nucleation and growth where growing cavities act as sources or sinks for the diffusion fields describing moving vacancies and interstitial atoms.^{14,15} Extended lattice defects absorb mobile point defect, too, reducing concentration of vacancies $c_v(\mathbf{r}, t)$ and interstitial atoms $c_i(\mathbf{r}, t)$ in the vicinity of each sink and suppressing both the nucleation and diffusional growth of cavities in the vicinity of each sink.

Clustering of defects in collision cascades brings a new important element in the dynamics of microstructural evolution of irradiated materials. The mobility of certain types of clusters of interstitial atoms produced in collision cascades turns out to be higher than that of point defects.¹⁶ As the

number of interstitial atoms in a cluster increases, its Brownian motion becomes nearly one dimensional. One dimensionally moving clusters are able to propagate in the atmosphere of randomly distributed lattice defects through larger distances than single vacancies or interstitial atoms. At the same time lattice defects affect the motion of one dimensionally diffusing clusters in a more substantial way than they influence the motion of single vacancies and interstitials since one dimensionally moving clusters cannot avoid obstacles by changing their direction of propagation.

It is in the dependence of the rate of growth of cavities on their size where the difference between contributions from diffusing point defects and from one dimensionally moving clusters manifests itself in the most notable way. For relatively small cavities growing by the attachment of vacancies, the rate $\dot{a}(t)$ of variation of cavity radius $a(t)$ is inversely proportional to $a(t)$, $\dot{a}(t) \sim 1/a(t)$, while the (negative) contribution to $\dot{a}(t)$ resulting from the bombardment of cavities by interstitial clusters exhibits no singularity as a function of $a(t)$. Given that extended lattice defects, for example, grain boundaries, affect the motion of point defects and defect clusters in a radically different way, we may expect that in the vicinity of those extended defects the growth of cavities is going to be characterized by features that are different from those characterizing the growth in the interior area of the grains. It has been observed experimentally^{17–19} that in the vicinity of grain boundaries the distribution of growing cavities becomes highly inhomogeneous. The growth of cavities is suppressed in the immediate vicinity of a grain boundary and the rate of growth is maximum at a certain distance from the boundary, decreasing again in the interior region of the grain. A theoretical model explaining the observed effects was proposed in Refs. 20 and 21 where the formation of the zone of inhomogeneous swelling was interpreted as being associated with the dependence of the swelling *rate* on the distance from the boundary. However, the model considered in^{20,21} neither takes into account the dependence of the rate of swelling on the size of growing cavities (where the size represents probably *the* most important parameter of the model²²) nor it accounts for the nucleation of new cavities. The significance of the latter effect stems

directly from experimental observations (see, e.g. Fig. 22 of Ref. 12).

In this paper we introduce a model describing the evolution of a population of cavities nucleating and growing in the vicinity of a planar sink and interacting with the binary diffusion field of single vacancies and interstitial atoms and with mobile interstitial clusters. We show that the competition between the nucleation and growth of cavities and the dependence of the rate of growth on the size of cavities gives rise to the formation of a zone of highly inhomogeneous swelling where at maximum the magnitude of swelling is up to eight times higher than that in the grain interior. We find that cavities growing near the grain boundary are able to reach substantially larger sizes than those growing in the interior area of the grain. We also show that the position of the peak of swelling depends on the density of growing cavities and that the distance between the peak and the boundary scales approximately as the inverse cubic root of the volume density of cavities, in agreement with experimental observations.

The paper is organized as follows. First we introduce a self-consistent set of equations describing the evolution of a spatially inhomogeneous distribution of growing cavities. Then we illustrate properties of these equations by analyzing several limiting cases where analytical treatment is possible. In what follows we develop a numerical scheme and investigate the self-consistent problem of inhomogeneous swelling of the material in the vicinity of a grain boundary. We compare the calculated swelling curves with those observed experimentally, and analyze the dependence of solutions of the model on parameters typically addressed in an experimental investigation of the problem.

II. THE MODEL

To characterize the population of cavities nucleating and growing in a spatially inhomogeneous system it is convenient to introduce the cavity size distribution function, which is a function of the cavity radius a , its coordinate \mathbf{r} and time t

$$f(a, \mathbf{r}, t) = \int_0^t \nu(\mathbf{r}, \tau) \delta[a - a(\mathbf{r}, t, \tau)] d\tau. \quad (1)$$

Here τ denotes the nucleation time, $a(\mathbf{r}, t, \tau)$ is the radius of a cavity nucleated at point \mathbf{r} at the moment $t = \tau$, and $\nu(\mathbf{r}, \tau)$ is the number of cavities nucleating per unit volume per unit time. Function (1) satisfies the normalization condition of the form

$$\int_0^\infty f(a, \mathbf{r}, t) da = \int_0^t \nu(\mathbf{r}, \tau) d\tau = N(\mathbf{r}, t),$$

where $N(\mathbf{r}, t)$ is the number density of growing cavities. Using Eq. (1) we find the total volume of cavities

$$S(\mathbf{r}, t) = \frac{4}{3} \pi \int_0^\infty a^3 f(a, \mathbf{r}, t) da = \frac{4}{3} \pi \int_0^t \nu(\mathbf{r}, \tau) a^3(\mathbf{r}, t, \tau) d\tau, \quad (2)$$

which is a dimensionless parameter characterizing the local swelling of the material. The swelling *rate* is found by the differentiation of Eq. (2)

$$\frac{dS(\mathbf{r}, t)}{dt} = 4\pi \int_0^t \nu(\mathbf{r}, \tau) a^2(\mathbf{r}, t, \tau) \frac{da(\mathbf{r}, t, \tau)}{dt} d\tau, \quad (3)$$

where it is taken into account that $a(\mathbf{r}, t, t) = 0$. Equation (3) shows that to characterize the magnitude of local swelling at point \mathbf{r} at time t we need to know the time dependence of the nucleation rate $\nu(\mathbf{r}, \tau)$ for $\tau \in [0, t]$ and also the equation describing the rate $\dot{a}(\mathbf{r}, t, \tau)$ of variation of the radius of a cavity nucleated at \mathbf{r} at $t = \tau$.

There are two competing processes giving rise to the variation of the radius of cavities considered as a function of time t . The first process is associated with the attachment to the surface of the cavity of single vacancies and interstitials, and the second one is due to the bombardment of growing cavities by mobile interstitial clusters, see e.g., Ref. 22,

$$\frac{da(\mathbf{r}, t, \tau)}{dt} = \left[\frac{da(\mathbf{r}, t, \tau)}{dt} \right]_{\text{point defects}} + \left[\frac{da(\mathbf{r}, t, \tau)}{dt} \right]_{\text{interst. clusters}}. \quad (4)$$

The first term in the right-hand side of Eq. (4) equals the difference between fluxes of single vacancies and interstitial atoms integrated over the surface of the cavity. For sufficiently large cavities (see Ref. 23 and Appendix A for more detail) this term can be expressed as

$$\left[\frac{da(\mathbf{r}, t, \tau)}{dt} \right]_{\text{point defects}} = \frac{1}{a(\mathbf{r}, t, \tau)} [D_v c_v(\mathbf{r}, t) - D_i c_i(\mathbf{r}, t)] \times \Theta(t - \tau), \quad (5)$$

where D_v and D_i are the diffusion coefficients ($D_v \ll D_i$) of vacancies and interstitials, respectively, and $c_v(\mathbf{r}, t)$ and $c_i(\mathbf{r}, t)$ are the local concentrations of vacancies and interstitial atoms. Function $\Theta(t - \tau)$ entering Eq. (5) is defined as $\Theta(t - \tau) = 1$ for $t \geq \tau$ and $\Theta(t - \tau) = 0$ for $t < \tau$.

The time-dependent concentrations of vacancies and interstitial atoms satisfy a system of two nonlinear equations describing the generation, diffusion, recombination and absorption of point defects in the presence of a sink

$$\begin{aligned} \frac{\partial}{\partial t} c_i(\mathbf{r}, t) &= D_i \frac{\partial^2}{\partial \mathbf{r}^2} c_i(\mathbf{r}, t) + K(1 - \epsilon) \\ &\quad - [Z_i \rho + \omega(\mathbf{r}, t)] D_i c_i(\mathbf{r}, t) - \alpha c_i(\mathbf{r}, t) c_v(\mathbf{r}, t) \\ &\quad - \sigma_i(\mathbf{r}, t), \\ \frac{\partial}{\partial t} c_v(\mathbf{r}, t) &= D_v \frac{\partial^2}{\partial \mathbf{r}^2} c_v(\mathbf{r}, t) + K - [Z_v \rho + \omega(\mathbf{r}, t)] D_v c_v(\mathbf{r}, t) \\ &\quad - \alpha c_i(\mathbf{r}, t) c_v(\mathbf{r}, t) - \sigma_v(\mathbf{r}, t). \end{aligned} \quad (6)$$

In these equations K is the effective rate of generation of point defects in the material by energetic particles and ρ is the density of randomly distributed dislocation lines. Dislocations absorb vacancies and interstitial atoms at slightly different rates, and this effect is described by the bias factors

$Z_i \sim 1$ and $Z_v \sim 1$, $Z_i > Z_v$. $\omega(\mathbf{r}, t)$ describes the absorption of point defects by growing cavities (an explicit expression for this term is derived in Appendix A) and α is the recombination constant. Here we are interested in following the evolution of the binary diffusion field $\{c_i(\mathbf{r}, t), c_v(\mathbf{r}, t)\}$ in the vicinity of an extended lattice defect (a grain boundary), and functions $\sigma_v(\mathbf{r}, t)$ and $\sigma_i(\mathbf{r}, t)$ represent the rates of absorption of vacancies and interstitial atoms by this defect.

Equations (6) show that the rates of generation of interstitial atoms and vacancies are unequal. This inequality is associated with the formation of clusters of interstitial atoms in collision cascades, and ϵ is the cluster formation ratio, $\epsilon \sim 1$.

The second term in Eq. (4) is associated with the bombardment of growing cavities by mobile interstitial clusters. To assess the contribution of this process to the rate of variation of the radius of growing cavities we need to average the flux of interstitial atoms transported by clusters to cavities over the positions and orientations of dislocation lines and over the coordinates of centres of cavities. For the case of *spatially homogeneous* distribution of cavities, where $a(z, t, \tau)$ is independent of z , the second term in Eq. (4) is given by

$$\left[\frac{da(t, \tau)}{dt} \right]_{\text{interst clusters}} = - \frac{K\epsilon}{\pi\rho d + 4\pi \int_0^t \nu(\tau') a^2(t, \tau') d\tau'} \times \Theta(t - \tau), \quad (7)$$

where d is the effective radius of absorption of one dimensionally moving clusters by dislocations. A more general expression valid for the case of a spatially inhomogeneous distribution of cavities near a plain grain boundary is derived in Appendix B. It has the form

$$\begin{aligned} \left[\frac{da(z, t, \tau)}{dt} \right]_{\text{interst clusters}} &= - \frac{K\epsilon}{8M} \Theta(t - \tau) \\ &\times \sum_{i=1}^M \left\{ \int_0^\infty \frac{dz'}{|\cos \gamma_i|} \exp \left[- \int_0^{z'} \frac{dz''}{|\cos \gamma_i|} \nu(z + z'', t) \right] \right. \\ &\left. + \int_0^z \frac{dz'}{|\cos \gamma_i|} \exp \left[- \int_0^{z'} \frac{dz''}{|\cos \gamma_i|} \nu(z - z'', t) \right] \right\}, \quad (8) \end{aligned}$$

where $\nu(z, t) = \pi/4\rho d + \pi \int_0^t \nu(\tau') a^2(z, t, \tau') d\tau'$ and summation is performed over possible directions of one-dimensional motion of interstitial clusters in a given crystal structure ($M=4$ for the bcc and $M=6$ for the fcc structure.²⁴) γ_i is the angle between the direction of motion of clusters and the z axis, which is assumed to be perpendicular to the plane of the grain boundary.

Expressions (1)–(8) form a closed self-consistent set of equations, the solution of which describes the evolution of a spatially inhomogeneous distribution of cavities nucleating and growing in the vicinity of a grain boundary in an irradiated material. Equations (1)–(8) describe the case where collision cascades lead to the formation of mobile clusters of

interstitial atoms. Analysis given below shows that clusterisation of interstitial atoms has a very significant effect on the evolution of the population of cavities. In particular, competition between growth by attachment of point defects to the surface of cavities and the bombardment of cavities by mobile interstitial clusters complemented by radically different transport properties of point defects and mobile clusters gives rise to a highly inhomogeneous pattern of swelling, where peak values are up to eight times higher than values characterizing swelling in the interior region of the grain.

III. ANALYSIS OF THE MODEL

A. Spatially homogeneous case

We start by considering a solution of Eqs. (1)–(8) corresponding to the case of spatially homogeneous distribution of cavities. The characteristic scale of spatial fluctuations of concentrations $c_i(\mathbf{r}, t)$ and $c_v(\mathbf{r}, t)$ equals $\tilde{z} \sim \rho^{-1/2}$ and therefore the temporal variation of concentrations is characterized by the time scale $\tilde{t} \sim (D\rho)^{-1} \sim 10$ s for $D \sim 10^{-9}$ cm²/s and $\rho \sim 10^8$ cm⁻². Since the time scale characterizing the growth of cavities is many times this value, the time derivatives of concentrations entering the left-hand side of Eq. (6) may be neglected. Assuming also that the defect production rate satisfies the condition $K \ll \rho D_i D_v / \alpha$, we neglect the recombination term and obtain

$$\begin{aligned} c_i(t) &= \frac{K(1-\epsilon)}{D_i} \left[\rho Z_i + 4\pi \int_0^t \nu(\tau') a(t, \tau') d\tau' \right]^{-1}, \\ c_v(t) &= \frac{K}{D_v} \left[\rho Z_v + 4\pi \int_0^t \nu(\tau') a(t, \tau') d\tau' \right]^{-1}. \quad (9) \end{aligned}$$

Combining Eqs. (9) and (5), we obtain the contribution to the rate of variation of the cavity radius associated with the flux of point defects arriving on its surface

$$\begin{aligned} \left[\frac{da(t, \tau)}{dt} \right]_{\text{point defects}} &= \frac{\Theta(t - \tau)}{a(t, \tau)} \\ &\times \left[\frac{K}{\rho Z_v + 4\pi \int_0^t \nu(\tau') a(t, \tau') d\tau'} \right. \\ &\left. - \frac{K(1-\epsilon)}{\rho Z_i + 4\pi \int_0^t \nu(\tau') a(t, \tau') d\tau'} \right]. \quad (10) \end{aligned}$$

In the case of instantaneous nucleation of cavities $\nu(t) = N_0 \delta(t)$ Eqs. (10) and (7) transform into equation²²

$$\begin{aligned} \frac{a(t, 0)}{dt} &= \frac{1}{a(t, 0)} \left[\frac{K}{\rho Z_v + 4\pi N_0 a(t, 0)} - \frac{K(1-\epsilon)}{\rho Z_i + 4\pi N_0 a(t, 0)} \right] \\ &- \frac{K\epsilon}{\pi\rho d + 4\pi N_0 a^2(t, 0)}. \quad (11) \end{aligned}$$

Depending on the choice of bias parameters Z_i, Z_v and the cluster formation ratio ϵ , solutions of Eq. (11) show two

radically different types of asymptotic behavior. One of them corresponds to the case where the growth of cavities eventually saturates, while the other describes growth which continues indefinitely as a function of irradiation time t . To investigate conditions corresponding to the crossover between these two scenarios we introduce dimensionless variables $\phi = Kt$, $\kappa = \rho d^2$, and $\chi_0 = N_0 d^3$. These variables have a simple meaning, namely, ϕ is the total irradiation dose (expressed in units of displacement per atom), κ is the measure of transparency of the dislocation network for one-dimensionally moving clusters, and χ_0 is the dimensionless volume density of growing cavities. Introducing also the dimensionless radius of cavities $r(\phi) = a(t, 0)/\pi d$, we obtain

$$\frac{dr}{d\phi} = \frac{1}{\pi^2 \kappa} \left[\frac{1}{r} \left(\frac{1}{Z_v + 4\pi^2 \chi_0 r / \kappa} - \frac{1 - \epsilon}{Z_i + 4\pi^2 \chi_0 r / \kappa} \right) - \frac{\epsilon}{1 + 4\pi^2 \chi_0 r^2 / \kappa} \right]. \quad (12)$$

Analysis of solutions of this equation given in Appendix C shows that in the case where $Z_i - Z_v > \epsilon Z_i$ and where the volume density of cavities is sufficiently large, the size of cavities given by Eq. (12) increases indefinitely in the limit of high irradiation dose as

$$r(\phi) \sim \frac{\kappa^{1/4}}{\sqrt{2\pi^3 \chi_0}^{1/2}} [Z_i - Z_v - \epsilon Z_i]^{1/4} \phi^{1/4}. \quad (13)$$

However, if $Z_i - Z_v \ll \epsilon Z_i$ then the growth of cavities saturates in the limit $\phi \rightarrow \infty$ at $r \approx 1$. Swelling of the material also saturates in this limit approaching the maximum value given by

$$S(\phi) = \frac{4}{3} \pi^4 \chi_0 r^3(\phi) |_{\max} \approx 1.3 \times 10^4 \chi_0 [\%]. \quad (14)$$

In most cases the cluster formation ratio ϵ is large (typically $\epsilon \sim 1$) in comparison with the difference between dislocation bias factors Z_i and Z_v [values of $(Z_i - Z_v)/Z_i$ lie in the interval between 1% and 3% (Ref. 25)]. This shows that keeping the dislocation bias terms in the model described above is unnecessary, and in what follows we only consider the case where $Z_i = Z_v = 1$.

B. Spatially inhomogeneous case

We now investigate solutions of Eqs. (1)–(8) describing the nucleation and growth of cavities in the vicinity of a grain boundary. The boundary is assumed to have the form of a plane situated at $z = 0$. This plane is able to absorb point defects and interstitial clusters that approach it. Since vacancies and interstitial atoms interact with grain boundaries via long-range elastic fields,²⁶ the rate of absorption of interstitial atoms by the boundary is expected to be higher than the rate of absorption of vacancies. However, in relative terms the interaction between point defects and grain boundaries is not as strong as it is between point defects and dislocations. Therefore, in order to ensure the consistency of our model, where the absorption of point defects by dislocations is assumed to be unbiased $Z_i = Z_v$, we must assume that there is

no difference in the effective rates of absorption of vacancies and interstitials by the grain boundary. In this case Eqs. (6) acquire the form

$$\begin{aligned} D_i \frac{d^2}{dz^2} c_i(z, t) + K(1 - \epsilon) - [\rho + \omega(z, t)] D_i c_i(z, t) \\ - \alpha c_i(z, t) c_v(z, t) = D_i c_i(z, t) \mathcal{Q} \delta(z), \\ D_v \frac{d^2}{dz^2} c_v(z, t) + K - [\rho + \omega(z, t)] D_v c_v(z, t) \\ - \alpha c_i(z, t) c_v(z, t) = D_v c_v(z, t) \mathcal{Q} \delta(z), \end{aligned} \quad (15)$$

where \mathcal{Q} characterizes the rate of absorption of point defects by the grain boundary. Since concentrations of vacancies and interstitial atoms enter Eq. (5) in the form of a linear combination $\Pi(z, t) = D_v c_v(z, t) - D_i c_i(z, t)$, we subtract the second of Eqs. (15) from the first one and obtain a closed equation on $\Pi(z, t)$

$$\frac{d^2}{dz^2} \Pi(z, t) + K\epsilon - [\rho + \omega(z, t)] \Pi(z, t) = \Pi(z, t) \mathcal{Q} \delta(z). \quad (16)$$

In the limit $\mathcal{Q} \rightarrow \infty$ the δ function term in the right-hand side of this equation is equivalent to the boundary condition $\Pi(0, t) = 0$.

We begin by considering the limit of low density of growing cavities $\omega(z, t) \ll \rho$. In this case Eq. (16) has stationary solution

$$\Pi(z) = \frac{K\epsilon}{\rho} (1 - e^{-\sqrt{\rho}z}). \quad (17)$$

Substituting this into Eq. (5), we arrive at

$$\left[\frac{da(z, t, \tau)}{dt} \right]_{\text{point defects}} = \frac{\Theta(t - \tau) K\epsilon}{a(z, t, \tau) \rho} [1 - \exp(-\sqrt{\rho}z)]. \quad (18)$$

In the limit of low density of cavities integration in Eq. (8) can be done analytically

$$\begin{aligned} \left[\frac{da(z, t, \tau)}{dt} \right]_{\text{interst. clusters}} \\ = - \frac{K\epsilon}{2\pi\rho d} \Theta(t - \tau) \left[2 - \frac{1}{M} \sum_{i=1}^M \exp\left(-\frac{\pi}{4} \frac{\rho d}{|\cos \gamma_i|} z\right) \right]. \end{aligned} \quad (19)$$

Combining Eqs. (18) and (19) we obtain that the radius of a cavity nucleated at distance z from the grain boundary at time τ satisfies the differential equation of the form

$$\begin{aligned} \frac{da(z, t, \tau)}{dt} = \frac{K\epsilon}{\rho} \Theta(t - \tau) \left\{ \frac{1 - \exp(-\sqrt{\rho}z)}{a(z, t, \tau)} - \frac{1}{2\pi d} \right. \\ \left. \times \left[2 - \frac{1}{M} \sum_{i=1}^M \exp\left(-\frac{\pi}{4} \frac{\rho d}{|\cos \gamma_i|} z\right) \right] \right\}. \end{aligned} \quad (20)$$

Initial condition for this equation is $a(z, \tau, \tau) = 0$.

If we assume that $a(z, t, \tau) = \pi d$ in the denominator of the first term in curly brackets in the right-hand side of Eq. (20), we obtain an equation which is similar to Eq. (15) of Ref. 20. The treatment developed in Ref. 20 is based on the assumption that the rate of growth of cavities near a grain boundary is independent of their size. This assumption is not consistent with the the initial condition $a(z, \tau, \tau) = 0$. Moreover, in the vicinity of a grain boundary the saturation radius $a(z, \infty, \tau)$ turns out to be a function of the distance z between the center of the cavity and the grain boundary. Therefore, to obtain a correct solution of Eq. (20) we have to retain the dependence of the right-hand side of this equation on the radius $a(z, t, \tau)$ of growing cavities.

Solution of Eq. (20) satisfying the appropriate initial condition can be represented in a parametric form as

$$a(z, t, \tau) + 2\pi d \frac{A(z)}{B(z)} \ln \left[1 - \frac{a(z, t, \tau)}{2\pi d} \frac{B(z)}{A(z)} \right] = -\Theta(t - \tau) \frac{K\epsilon}{2\pi\rho d} B(z)(t - \tau), \quad (21)$$

where $A(z)$ and $B(z)$ are dimensionless functions of z given by

$$A(z) = 1 - \exp(-\sqrt{\rho}z),$$

and

$$B(z) = 2 - \frac{1}{M} \sum_{i=1}^M \exp\left(-\frac{\pi}{4} \frac{\rho d}{|\cos \gamma_i|} z\right).$$

Formula (21) shows that at small $t - \tau \ll \rho d^2 / K\epsilon$ the radius of the growing cavity increases as the square root of the time elapsed from the moment of nucleation

$$a(z, t, \tau) = \Theta(t - \tau) \sqrt{\frac{2K\epsilon}{\rho} A(z)(t - \tau)}. \quad (22)$$

Therefore, the rate of growth of cavities at small times is independent of the second term in the right-hand side of Eq. (20), or, in other words, the growth of small cavities is not affected by the bombardment of cavities by one dimensionally moving interstitial clusters. Mathematically, this is a simple corollary of the fact that the first term in the right-hand side of Eq. (20) is singular in the limit $a(z, t, \tau) \rightarrow 0$.

For large $t - \tau \gg \rho d^2 / K\epsilon$ the growth of cavities saturates and their radius $a(z, t, \tau)$ approaches the maximum value given by

$$\lim_{t - \tau \rightarrow \infty} a(z, t, \tau) = a_{\max}(z) = 2\pi d \frac{A(z)}{B(z)}. \quad (23)$$

This equation shows that for $z = z^* \sim \rho^{-1/2}$ and $\rho d^2 \ll 1$ cavities are able to reach size $a_{\max}(z^*) = 2\pi d$, which is twice the maximum size $a_{\max} = \pi d$ that cavities reach in the interior region of the grain. This implies that the peak value of swelling of the material in the vicinity of a grain boundary can be up to eight times higher than the maximum value characterizing swelling in the grain interior.

Figure 1 shows the dependence of the saturation radius $a_{\max}(z)$ on the distance z from the grain boundary. Cavities growing near a grain boundary can reach substantially larger

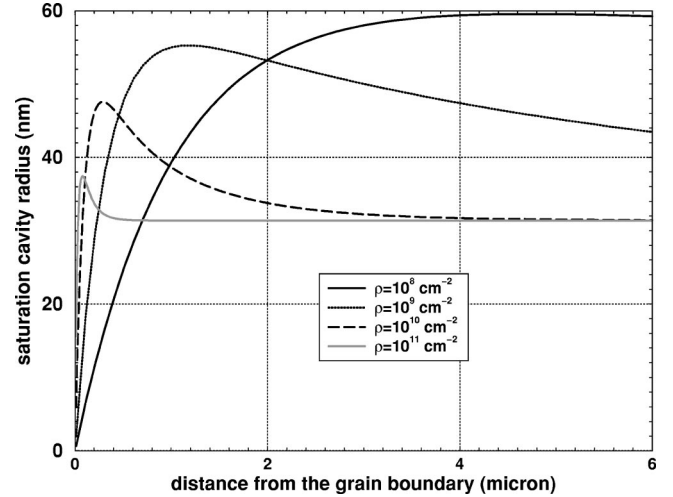


FIG. 1. Dependence of the saturation radius $a_{\max}(z)$ of cavities nucleated at distance z from a grain boundary in an irradiated material. Calculations were performed for several values of the dislocation density ρ spanning from $\rho = 10^8 \text{ cm}^{-2}$ (a well annealed material) to a high dislocation density material characterized by $\rho = 10^{11} \text{ cm}^{-2}$. The effective radius of absorption of interstitial clusters by dislocations d is assumed to be equal to 10 nm, and the saturation radius of cavities growing in the interior region of the grain πd equals 31.4 nm.

sizes than cavities growing in the grain interior (for $d = 10 \text{ nm}$ the saturation radius of cavities growing in the interior region of the grain is approximately equal to 31.4 nm). The position of the peak of swelling z^* corresponding to the maximum of function $a_{\max}(z)$ decreases monotonically as a function of the density of dislocation lines ρ .

Equations (18)–(20) describe the case where the volume density of growing cavities was assumed to be low. In this case dislocations are primarily responsible for the absorption of mobile point defects and interstitial clusters, and the effect of nonlinear terms describing the influence of the “atmosphere” of growing cavities on the rate of cavity growth is negligible. In the next section we investigate the part played by these nonlinear terms and the limit of high density of growing cavities.

C. Nucleation of cavities and the high density limit

In this section we study solutions of a general nonlinear self-consistent system of equations describing the nucleation and growth of cavities near a grain boundary. If the volume density of cavities exceeds the limit defined by the condition $4\pi \int_0^1 \nu(z, \tau) a(z, t, \tau) d\tau = \rho$, the approach described in the preceding section is no longer valid and the presence of cavities affects concentrations of freely moving vacancies and interstitial atoms. Furthermore, if the volume density of cavities is large enough so that $\pi \int_0^1 \nu(z, \tau') a^2(z, t, \tau') d\tau \gg (\pi/4)\rho d$, the one-dimensional motion of interstitial clusters is also affected by their interaction with cavities. In this case integral (8) can no longer be approximated by expression (19) corresponding to the low cavity density limit.

To investigate the high-density case we introduce an additional simplifying approximation in our model (1)–(8). In-

stead of performing summation over directions of motion of interstitial clusters in the crystal lattice, we introduce an average quantity $\langle \cos \gamma \rangle$ characterizing the “average” angle between the direction of motion of clusters and the z axis.

Using dimensionless variables, we obtain equations describing how the radius of a cavity growing in a dense spatially inhomogeneous environment varies with the irradiation dose ϕ .

$$\begin{aligned} \frac{d}{d\phi} r(\zeta, \phi, \phi') = & \Theta(\phi - \phi') \frac{\epsilon}{\pi^2 \kappa} \left\{ \frac{\Pi(\zeta, \phi)}{r(\zeta, \phi, \phi')} - \frac{1}{2} \int_0^\infty \frac{d\zeta'}{\langle \cos \gamma \rangle} \exp \left[- \int_0^{\zeta'} \frac{d\zeta''}{\langle \cos \gamma \rangle} \left(1 + \frac{4\pi^2}{\kappa} \int_0^\phi d\phi'' \chi(\zeta + \zeta'', \phi'') \right. \right. \right. \\ & \left. \left. \left. \times r^2(\zeta + \zeta'', \phi, \phi'') \right) \right] - \frac{1}{2} \int_0^\zeta \frac{d\zeta'}{\langle \cos \gamma \rangle} \exp \left[- \int_0^{\zeta'} \frac{d\zeta''}{\langle \cos \gamma \rangle} \left(1 + \frac{4\pi^2}{\kappa} \int_0^\phi d\phi'' \chi(\zeta - \zeta'', \phi'') r^2(\zeta - \zeta'', \phi, \phi'') \right) \right] \right\}. \end{aligned} \quad (24)$$

Here $\phi = Kt$ is the irradiation dose and $\phi' = K\tau$ is the dose corresponding to the moment of nucleation. $\zeta = (\pi/4)z\rho d$ is the dimensionless distance between the cavity and the grain boundary. $\chi(\zeta, \phi') = (K/d^3)\nu(z, \tau)$ is the dimensionless cavity nucleation rate, and $\kappa = \rho d^2$ is the parameter characterizing the transparency of the dislocation atmosphere for one-dimensionally moving clusters. $r(\zeta, \phi, \phi')$ is the cavity radius expressed in units πd , and function $\Pi(\zeta, \phi)$ satisfies equation

$$\begin{aligned} \frac{\pi^2}{16} \kappa \frac{d^2}{d\zeta^2} \Pi(\zeta, \phi) + 1 \\ - \left[1 + \frac{4\pi^2}{\kappa} \int_0^\phi d\phi'' \chi(\zeta, \phi'') r(\zeta, \phi, \phi'') \right] \Pi(\zeta, \phi) \\ = 0. \end{aligned} \quad (25)$$

The boundary condition for Eq. (25) has the form $\Pi(0, \phi) = 0$. The magnitude of local swelling associated with cavities nucleating and growing at distance ζ from the grain boundary is related to the solution of Eq. (24) via

$$S(\zeta, \phi) = \frac{4}{3} \pi^4 \int_0^\phi d\phi' \chi(\zeta, \phi') r^3(\zeta, \phi, \phi'). \quad (26)$$

Equation (24) has a simple meaning. It shows that the rate of growth of a cavity situated at point ζ is proportional to the difference between two terms, where the first one is singular in $r(\zeta, \phi, \phi')$ and describes diffusional growth by the attachment of single vacancies and interstitial atoms. The second term (which itself is a sum of two integrals) describes collisions between the cavity and gliding interstitial clusters.

The evaluation of the first term in Eq. (24) requires solving inhomogeneous diffusion equation (25) for a dimensionless function $\Pi(\zeta, \phi)$, which describes the dependence of the concentration of point defects on the distance from the grain boundary. A rigorous approach to solving Eq. (25) is described in Appendix D. A detailed analysis of numerical solutions of Eq. (25) shows that these solutions may be approximated by expression

$$\begin{aligned} \Pi(\zeta, \phi) = & \frac{1}{1 + \frac{4\pi^2}{\kappa} \int_0^\phi d\phi'' \chi(\zeta, \phi'') r(\zeta, \phi, \phi'')} \\ & \times \left\{ 1 - \exp \left(- \frac{4\zeta}{\pi\sqrt{\kappa}} \left[1 + \frac{4\pi^2}{\kappa} \right. \right. \right. \\ & \left. \left. \left. \times \int_0^\phi d\phi'' \chi(\zeta, \phi'') r(\zeta, \phi, \phi'') \right]^{1/2} \right) \right\}. \end{aligned} \quad (27)$$

Numerical evaluation of integrals in Eq. (24) can be performed using finite difference algorithms.²⁷ The fact that the asymptotic behavior of the radius of growing cavities in the grain interior is known from the solution of Eq. (10) makes it possible to evaluate the tails of integral terms analytically therefore avoiding lengthy numerical integration over a large range of variation of variables ζ'' and ζ' . According to the classical theory of nucleation,²⁸⁻³⁰ the rate of nucleation of cavities $\chi(\zeta, \phi)$ is a functional of the local concentration of vacancies. In what follows we assume that the rate of nucleation has the form $\chi(\zeta, \phi) = \bar{\chi} \Pi^h(\zeta, \phi)$, where $\bar{\chi}$ is a constant and h is an integer. This simple approximation makes it possible to investigate a number of cases ranging from the limit of continuous nucleation corresponding to $h=0$, to the limit of almost instantaneous nucleation of cavities at the onset of growth, $h \gg 1$.

We begin by investigating the instantaneous nucleation case where all the cavities are assumed to nucleate at $t=0$. This case corresponds to $\chi(\zeta, \phi) = \chi_0 \delta(\phi)$. The volume density of cavities in this case remains constant and independent of either the dose ϕ or the distance ζ . The formation of spatially inhomogeneous profile of swelling in this case is associated entirely with the fact that the rate of growth of cavities depends on the distance ζ from the boundary.

Figure 2 illustrates the formation and the development of profiles of inhomogeneous swelling $S = S(\zeta, \phi)$ in the vicinity of a grain boundary. At any given dose ϕ the profile has a characteristic shape with a maximum situated at a certain characteristic distance ζ^* from the boundary. This distance ζ^* , considered as a function of the dose ϕ , decreases monotonically with increasing ϕ . This agrees well with experimental observations.¹²

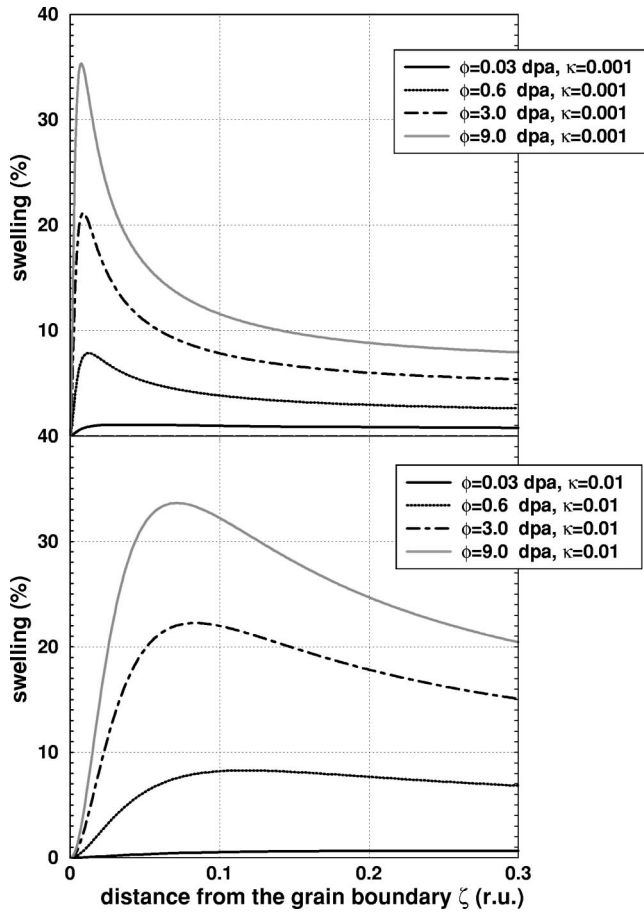


FIG. 2. Profiles of inhomogeneous swelling near a grain boundary calculated for the high cavity density case assuming spatially homogeneous and instantaneous nucleation of cavities. Curves shown in the upper part of the figure correspond to lower density of dislocations than the curves shown in the lower part of the figure. Note the high values of swelling characterizing the growth of cavities in the vicinity of the grain boundary. Calculations were performed using Eqs. (24)–(27) for $\epsilon=0.6$, $\langle \cos \gamma \rangle=0.8$, and $\chi_0=0.001$.

In all the cases investigated in this work swelling profiles exhibited saturation in the limit of large irradiation doses ϕ . For $\phi \gg 1$ any further increase of the dose results in no change either in the magnitude of swelling or in the shape of the swelling profile. This result is entirely consistent with Eqs. (24)–(27). Integrals over ϕ entering Eqs. (24) and (26) for the instantaneous nucleation case are proportional to the radius of cavities. Since the radius of cavities saturates in the limit $t \rightarrow \infty$, so does the swelling profile. The dose ϕ required to reach saturation tends to be smaller in the case of low density of dislocations (very small values of κ) in comparison with the case of high dislocation density (intermediate values of κ).

An interesting question that we can now address on the basis of the model described above concerns the dependence of the position ζ^* of the peak of swelling on the volume density of growing cavities. In the case where the nucleation of voids is assumed to be instantaneous, the volume density of cavities N_0 is related to χ_0 via $\chi_0=N_0d^3$. Equations (24)–(27) show that the behavior that the model exhibits as a function of χ_0 becomes highly nonlinear for $\chi_0 > \kappa/2\pi$. To

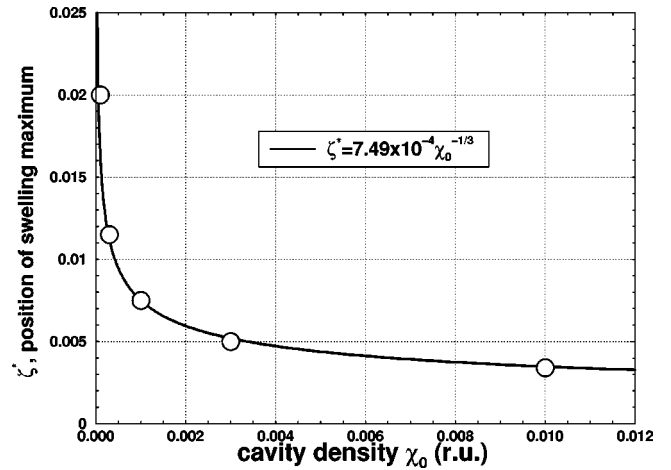


FIG. 3. Dependence of the position of the maximum of the swelling curve ζ^* on the dimensionless volume density $\chi_0=N_0d^3$ of cavities. Numerical calculations were performed using Eqs. (24)–(27) for $\epsilon=0.6$, $\langle \cos \gamma \rangle=0.8$, and $\kappa=0.001$. The solid line is a power-law fit to the set of points calculated numerically.

investigate the functional dependence $\zeta^*(\chi_0)$ in this case we have to refer to numerical solutions of the model similar to those shown in Fig. 2.

Figure 3 illustrates the dependence of the position of the maximum of the swelling curve on the volume density of growing cavities. In the limit of small densities $\chi_0 \ll \kappa/2\pi$ the coordinate of the maximum ζ^* is nearly independent on the density of cavities. However, in the case where $\chi_0 \gg \kappa/2\pi$ the dependence of ζ^* on χ_0 proves to be very strong. Approximating the function $\zeta^*(\chi_0)$ by a power law we obtain that the best fit is given by $\zeta^* \sim \chi_0^{-1/3}$. In dimensional units this is equivalent to $z^* \sim N_0^{-1/3}$, or, in other words, the distance between the peak of swelling and the grain-boundary scales approximately as the average distance between the cavities. This type of scaling is very similar to the one observed experimentally.¹⁹

So far in this section we have been studying the case of instantaneous nucleation of cavities. Now we consider the case where cavities continue to nucleate even after the onset of growth. In the case where the nucleation of cavities proceeds in parallel with their growth, Eqs. (24)–(27) become nonlocal only in space, but also in time. Formally, this nonlocality manifests itself in the form of the appearance in Eq. (24) of two types of integral terms. Integrals over ζ describe the nonlocality associated with the long-range transport of interstitial atoms by mobile clusters. The second type of nonlocality is the temporal nonlocality, which is associated with the fact that the growth of cavities nucleated at a certain moment of time τ (corresponding to a certain value of the irradiation dose $\phi' = K\tau$) is affected by the presence of cavities nucleated at earlier times $t \leq \tau$. This means that at an any given time the population of cavities at a given distance ζ from the grain boundary is characterized by a distribution of sizes rather than by a certain value of their radius.

Figure 4 illustrates the effect of the mode of nucleation of cavities on the shape of the swelling curve. Continuous nucleation of cavities (curves shown in the left column) tends to lead to higher swelling than that obtained in the case where the initial sharp drop in the concentration of vacancies

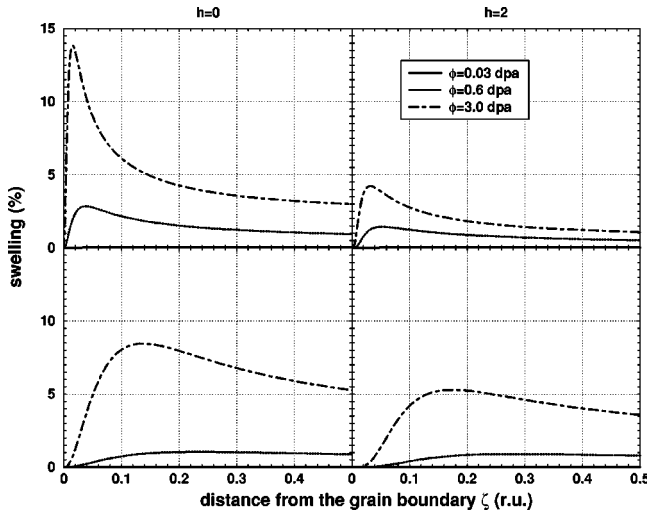


FIG. 4. Profiles of inhomogeneous swelling calculated for the case of continuous nucleation of cavities. The rate of nucleation of cavities was assumed to be proportional to the concentration of vacancies $\chi(\zeta, \phi) = \bar{\chi} \Pi^h(\zeta, \phi)$. All the curves shown in this figure were calculated for $\bar{\chi} = 10^{-4}$. Profiles shown in the top row were calculated for $\kappa = 0.001$. Profiles shown below correspond to $\kappa = 0.01$.

suppresses further nucleation of cavities (curves shown in the right column). The shape of the curve depends on a number of parameters including the density of dislocation and the dose, and also on the volume density of cavities accumulated over the time elapsed since the onset of growth.

In Fig. 5 we compare swelling profiles calculated using Eqs. (24)–(27) in the continuous nucleation approximation and profiles observed experimentally. Experimental data re-

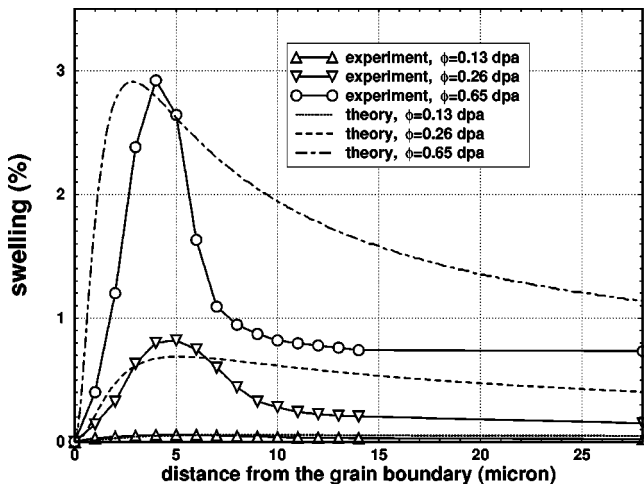


FIG. 5. Comparison between swelling profiles measured experimentally (see Fig. 22 in Ref. [12]) and calculated numerically using Eqs. (24)–(27). Calculations were performed assuming $\bar{\chi} = 1.2 \times 10^{-4}$, $\kappa = 0.001$, $h = 0$, and $\epsilon = 0.6$. The incubation dose corresponding to the onset of growth was assumed to be equal to 0.08 dpa. The asymmetry of the calculated profiles is associated with the difference between the spatial scales characterizing the diffusion of point defects and the one-dimensional Brownian motion of interstitial clusters, and also with the effect of saturation of swelling in the grain interior.

ported in Ref. 12 indicate that swelling was accompanied by the continuous nucleation of new cavities, and the latter effect was taken into account in the calculations. Both the scale of the curves and the position of maxima of experimentally measured and calculated profiles agree reasonably well. At the same time Fig. 5 shows the presence of a notable deviation of calculated profiles from experimental data in the region of large z , where the tails of calculated profiles decrease more slowly than the tails of profiles measured experimentally. This effect reflects the presence of a somewhat higher degree of absorption of mobile interstitial clusters in the interior region of the grain than that predicted by Eqs. (24)–(27). It is possible to speculate that the additional contribution to the absorption coefficient may come from scattering by immobile interstitial clusters, but the exact microscopic origin of the phenomenon remains unclear.

The fact that cavities continue to nucleate after the onset of growth leads to the situation where at any given irradiation dose ϕ the population of cavities is characterized by a relatively wide distribution of sizes. At any given moment of time this distribution can be found using formula (1). The presence of the δ -function term in Eq. (1) makes this formula somewhat inconvenient for numerical calculations. However, the difficulties can be readily circumvented by replacing the integral by a sum over a finite number of points, and by approximating the δ function by the Kronecker δ symbol. Figure 6 shows cavity size distributions corresponding to three different distances between the point z , where the size distribution is evaluated, and the grain boundary. All three distributions correspond to the swelling profile shown in Fig. 5 by the dash-dotted line. The shape of all the distributions turns out to be remarkably similar and nonanalytic $f(a, z) \sim [a_{\max}(z) - a]^{-1}$. The presence of a sharp peak on the right edge of all distributions is associated with the fact that the radius of cavities saturates in the limit of large doses. This point shows that an experimental investigation of the distribution of cavities as a function of their size may offer an interesting insight into the microscopic mechanisms of their formation and growth.

IV. SUMMARY

In this paper we investigated the formation and development of profiles of spatially inhomogeneous growth of cavities near a planar lattice defect (a grain boundary). The model describes both the nucleation and growth of cavities, and takes into account competing processes of diffusional growth of cavities by the attachment of point defects and the destruction of cavities in collisions with interstitial clusters. The model shows the formation of a characteristic profile of inhomogeneous swelling, where the maximum of the profile drifts towards the grain boundary as a function of time. Cavities growing in the vicinity of a grain boundary are shown to be able to reach substantially larger sizes than cavities growing in the interior region of the grain. The magnitude of swelling at maximum is found to be up to eight times higher than the value characterizing swelling in the grain interior. Profiles calculated numerically by solving the nonlinear self-consistent equations describing the evolution of the spatially inhomogeneous population of cavities are shown to compare well with profiles measured experimentally. The position z^*

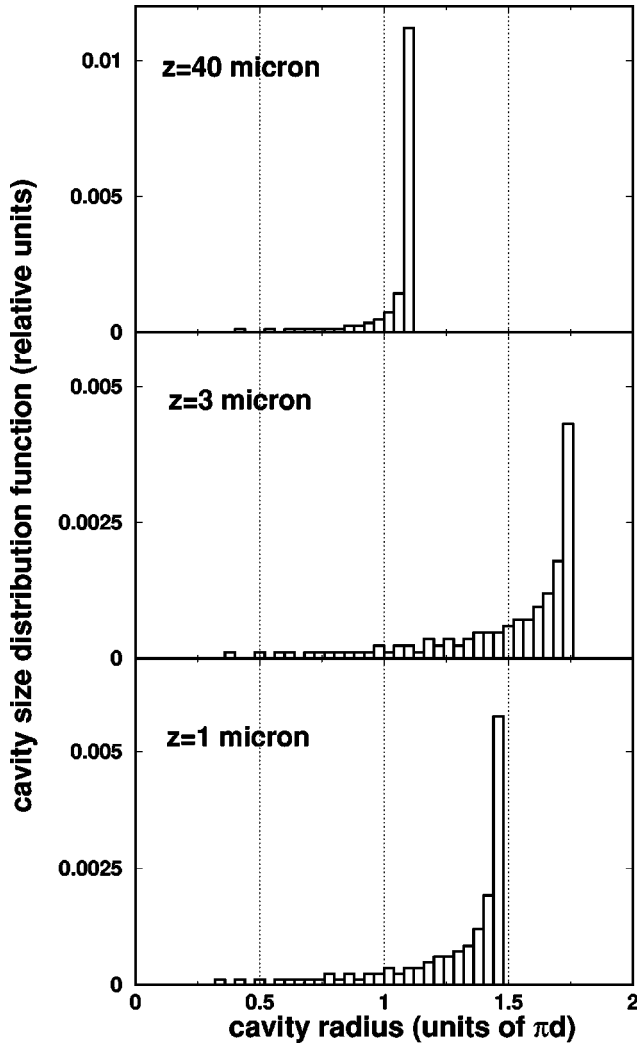


FIG. 6. Distribution of sizes of cavities nucleated and grown in the vicinity of a grain boundary. Calculations were performed for the same values of parameters as those used in Fig. 5. The irradiation dose $\phi=0.65$ dpa. Note that the growth of cavities in the interior region of the grain saturates at $a/\pi d=1$.

of the maximum of swelling profiles is found to scale with the density of cavities N_0 as $z^* \sim N_0^{-1/3}$ in agreement with experimental observations.

ACKNOWLEDGMENTS

The author wishes to acknowledge stimulating discussions with M. L. Jenkins, J. R. Matthews, Yu. N. Osetsky, A. A. Semenov, B. N. Singh, A. M. Stoneham, A. P. Sutton, M. Victoria, and C. H. Woo. The author is grateful to Ian Cook for comments and suggestions. This work was jointly funded by the UK Department of Trade and Industry and by EURATOM.

APPENDIX A

To evaluate the rate of absorption of point defects by randomly distributed cavities we consider an inhomogeneous diffusion equation

$$D \frac{\partial^2}{\partial \mathbf{r}^2} G(\mathbf{r}, \mathbf{r}') = \delta(\mathbf{r} - \mathbf{r}'), \quad (\text{A1})$$

the solution of which is

$$G(\mathbf{r}, \mathbf{r}') = - \frac{1}{4\pi D |\mathbf{r} - \mathbf{r}'|}. \quad (\text{A2})$$

Consider a spherical cavity of radius a growing by the attachment of diffusing particles to its surface. The concentration of diffusing particles around the cavity is given by²³

$$c(\mathbf{r}) = c_\infty - \frac{a}{r} \frac{(av/D)}{1 + (av/D)} [c_\infty - c^{(eq)}(a)], \quad (\text{A3})$$

where v is the effective velocity, which is a parameter entering the boundary condition for the rate of attachment of particles to the surface of the cavity

$$D \frac{\partial c}{\partial r} \Big|_{r=a} = v [c_\infty - c^{(eq)}(a)]. \quad (\text{A4})$$

Generalizing Eq. (A3) to the case of a weakly inhomogeneous distribution of diffusing particles, we arrive at

$$c(\mathbf{r}) = c_0(\mathbf{r}) + 4\pi D a \frac{(av/D)}{1 + (av/D)} \int d\mathbf{R} d\mathbf{r}' G(\mathbf{r} - \mathbf{R}) \times \delta(\mathbf{R} - \mathbf{r}') [c_0(\mathbf{R}) - c^{(eq)}(a)], \quad (\text{A5})$$

where \mathbf{r}' is the coordinate of the center of the cavity and $c_0(\mathbf{r})$ is the diffusion field corresponding to the case where the perturbation associated with the cavity may be neglected. In what follows we assume that the average concentration of diffusing particles is many times their equilibrium concentration $c^{(eq)}(a)$. In this case the evaporation term in the right-hand side of Eq. (A5) may be neglected and this equation becomes identical to the equation defining the T matrix in the theory of scattering^{31,32}

$$\psi(\mathbf{r}) = \psi_0(\mathbf{r}) + \int d\mathbf{R} d\mathbf{r}' G(\mathbf{r} - \mathbf{R}) T(\mathbf{R}, \mathbf{r}') \psi_0(\mathbf{r}'). \quad (\text{A6})$$

To average Eq. (A5) over the positions of centres of cavities we now follow the procedure developed for Eq. (A6) by Lax^{33,34} and obtain

$$c(\mathbf{r}) = c_0(\mathbf{r}) + 4\pi D a \frac{(av/D)}{1 + (av/D)} \int d\mathbf{r}' G(\mathbf{r} - \mathbf{r}') f(\mathbf{r}') c(\mathbf{r}'), \quad (\text{A7})$$

where $f(\mathbf{r}')$ is the volume density of cavities at point \mathbf{r}' . Representing this function in the form of the integral over the cavity size distribution function $f(a, \mathbf{r}')$ as $f(\mathbf{r}') = \int_0^\infty da f(a, \mathbf{r}')$, we arrive at

$$c(\mathbf{r}) = c_0(\mathbf{r}) + 4\pi D \int_0^\infty da a \frac{(av/D)}{1 + (av/D)} \int d\mathbf{r}' \times G(\mathbf{r} - \mathbf{r}') f(a, \mathbf{r}') c(\mathbf{r}'). \quad (\text{A8})$$

Finally, acting on both sides of this equation by operator $D(\partial^2/\partial \mathbf{r}^2)$ and comparing the result with Eq. (6), we find

$$\omega(\mathbf{r}, t) = 4\pi \int_0^\infty da a \frac{(av/D)}{1+(av/D)} f(a, \mathbf{r}, t). \quad (\text{A9})$$

Combining Eqs. (1) and (A9), we obtain

$$\omega(\mathbf{r}, t) = 4\pi \int_0^t \nu(\mathbf{r}, \tau) a(\mathbf{r}, t, \tau) \frac{[a(\mathbf{r}, t, \tau)v/D]}{1+[a(\mathbf{r}, t, \tau)v/D]} d\tau. \quad (\text{A10})$$

As the radius of the growing cavity increases (in practice this means that the cavity contains more than just a few atoms) we approach the limit $a(\mathbf{r}, t, \tau)v/D \gg 1$ where Eq. (A10) can be further simplified as

$$\omega(\mathbf{r}, t) = 4\pi \int_0^t \nu(\mathbf{r}, \tau) a(\mathbf{r}, t, \tau) d\tau. \quad (\text{A11})$$

This limit corresponds to the expression for the rate of growth given by Eq. (5).

APPENDIX B

In this Appendix we show how to derive Eq. (8) describing the (negative) contribution to the rate of growth of cavities due to the bombardment of cavities by one dimensionally moving interstitial clusters. We assume that *all* the interstitial clusters produced in collision cascades are glissile.

Consider a problem of one-dimensional motion of a particle along the z axis. We assume that the particle encounters obstacles that are distributed along the z axis with density $n(z)$. In other words, $n(z)dz$ is the total number of obstacles situated between z and $z+dz$. Consider now an arbitrary point z_0 . The probability $P_R(X_R, z_0)$ of finding the nearest to z_0 obstacle at a certain distance X_R from z_0 in the positive direction of the z axis (i.e., on the right of z_0), is given by the solution of equation

$$P_R(X_R, z_0) = \left(1 - \int_0^{X_R} P_R(X', z_0) dX' \right) n(z_0 + X_R). \quad (\text{B1})$$

We assume that the density of obstacles does not vanish in the limit $X_R \rightarrow \infty$ and therefore $\lim_{X_R \rightarrow \infty} \int_0^{X_R} dX' n(z_0 + X') = \infty$. In this case we can transform integral Eq. (B1) into a differential equation

$$\frac{d}{dx} \left(\frac{P_R(X_R, z_0)}{n(z_0 + X_R)} \right) = -n(z_0 + X_R) \left(\frac{P_R(X_R, z_0)}{n(z_0 + X_R)} \right), \quad (\text{B2})$$

and obtain

$$P_R(X_R, z_0) = n(z_0 + X_R) \exp \left(- \int_0^{X_R} dX' n(z_0 + X') \right). \quad (\text{B3})$$

To prove that this probability distribution is normalized we integrate $P_R(X_R, z_0)$ over a semi-infinite interval of variation of X_R and obtain

$$\int_0^\infty dX_R n(z_0 + X_R) \exp \left(- \int_0^{X_R} dX' n(z_0 + X') \right) = 1. \quad (\text{B4})$$

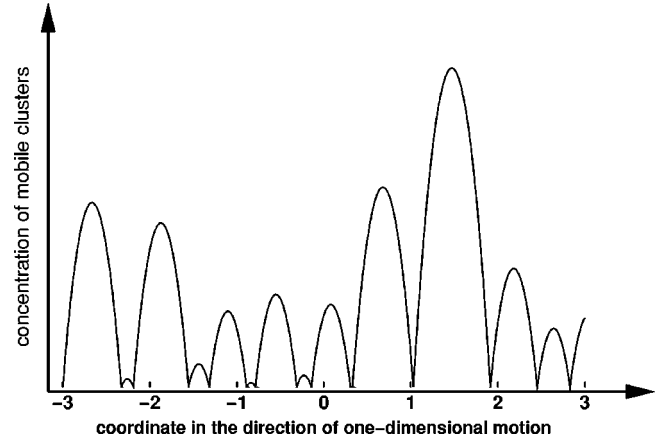


FIG. 7. Sketch illustrating the solution (B6) of the diffusion equation describing the one-dimensional Brownian motion of mobile interstitial clusters.

Similarly, the probability of finding an obstacle that the nearest to z_0 and that is situated on the left-hand side of z_0 at a distance X_L , is given by

$$P_L(X_L, z_0) = n(z_0 - X_L) \exp \left(- \int_0^{X_L} dX' n(z_0 - X') \right). \quad (\text{B5})$$

The concentration $C(z)$ of particles moving along the z axis in a *given* configuration if obstacles situated at points $z_1, z_2 \dots z_N \dots$ is given by the solution of the time-independent diffusion equation

$$D \frac{d^2}{dz^2} C(z) + K_c = 0$$

satisfying boundary conditions of the form $C(z_1) = C(z_2) = \dots = C(z_N) \dots = 0$. This solution has the form

$$C(z) = \frac{K_c}{2D} [(z - z_1)(z_2 - z) \Theta(z - z_1) \Theta(z_2 - z) + (z - z_2)(z_3 - z) \Theta(z - z_2) \Theta(z_3 - z) + \dots]. \quad (\text{B6})$$

A graphical illustration of Eq. (B6) is given in Fig. 7. The average concentration of particles at a certain point z equals

$$\langle C(z) \rangle = \frac{K_c}{2D} \langle (z - z_L)(z_R - z) \rangle = \frac{K_c}{2D} \langle X_L \rangle \langle X_R \rangle. \quad (\text{B7})$$

Taking into account the fact that

$$\begin{aligned} \langle X_R \rangle &= \int_0^\infty dX X n(z + X) \exp \left(- \int_0^X dX' n(z + X') \right) \\ &= \int_0^\infty dX X \left[- \frac{d}{dX} \exp \left(- \int_0^X dX' n(z + X') \right) \right] \\ &= \int_0^\infty dX \exp \left(- \int_0^X dX' n(z + X') \right), \end{aligned} \quad (\text{B8})$$

and deriving a similar expression for $\langle X_L \rangle$, we obtain

$$\langle C(z) \rangle = \frac{K_c}{2D} \left[\int_0^\infty dX \exp\left(-\int_0^X dX' n(z+X')\right) \right] \times \left[\int_0^\infty dX \exp\left(-\int_0^X dX' n(z-X')\right) \right]. \quad (\text{B9})$$

We now consider how to evaluate the probability of finding an obstacle that is the nearest to a given point $z_0 > 0$ in a configuration where the position of the obstacle situated at $z=0$ is stationary. In this case the expression for $P_R(X_R, z_0)$ remains unchanged but instead of Eq. (B5) we obtain

$$P_L(X_L, z_0) = n(z_0 - X_L) \exp\left(-\int_0^{X_L} dX' n(z_0 - X')\right) + \delta(z_0 - X_L) \exp\left(-\int_0^{z_0} dX' n(z_0 - X')\right). \quad (\text{B10})$$

The average concentration of moving particles is now given by

$$\langle C(z) \rangle = \frac{K_c}{2D} \left[\int_0^\infty dX \exp\left(-\int_0^X dX' n(z+X')\right) \right] \times \left[\int_0^z dX \exp\left(-\int_0^X dX' n(z-X')\right) \right]. \quad (\text{B11})$$

For example, in the case where $n(z) = n_0 = \text{const}$ we obtain

$$\langle C(z) \rangle = \frac{K_c}{2Dn_0^2} [1 - \exp(-n_0 z)]. \quad (\text{B12})$$

Now consider the solution of Eq. (B7) on a given interval $[z_L, z_R]$. If we place an absorbing probe at a point $z \in [z_L, z_R]$ and calculate the total flux J of particles towards this probe from the both sides of the interval, we find that

$$J = D \frac{d}{dz} C(z)|_{z=0} - D \frac{d}{dz} C(z)|_{z=0} = \frac{K_c}{2} (z_R - z_L) = \frac{K_c}{2} (X_R + X_L), \quad (\text{B13})$$

where $X_R = z_R - z$ and $X_L = z - z_L$ are the distances to obstacles that are nearest to the probe located at point z . Integrating Eq. (B13) with probability distributions (B3) and (B10), we arrive at

$$\langle J \rangle = \frac{K_c}{2} \left[\int_0^\infty dX \exp\left(-\int_0^X dX' n(z+X')\right) + \int_0^z dX \exp\left(-\int_0^X dX' n(z-X')\right) \right]. \quad (\text{B14})$$

To establish a connection between Eq. (B14) and the rate of

variation of the radius of a cavity we note that the effective production rate K_c of interstitial atoms moving one-dimensionally as a part of gliding clusters, is related to the volume production rate of clusters via (note that all the interstitial clusters produced in collision cascades are assumed to be glissile)

$$K_c = \frac{K \epsilon s_\perp}{M a_0^3}, \quad (\text{B15})$$

where M is the number of possible directions of one-dimensional motion in a crystal lattice of a given symmetry, a_0 is the lattice constant and s_\perp is the area of the projection of the Wigner-Seitz cell on the chosen direction of one-dimensional motion.

Now consider a spherical cavity containing \mathcal{N} vacancies. The volume of the cavity is equal to

$$\mathcal{N} a_0^3 = \frac{4}{3} \pi a^3(t). \quad (\text{B16})$$

The rate of variation of the number of vacancies in a cavity is related to the current of interstitials via

$$\frac{d\mathcal{N}}{dt} = -\langle J \rangle \frac{\pi a^2(t)}{s_\perp}. \quad (\text{B17})$$

Multiplying both sides of this equation by a_0^3 and noting that

$$\frac{d}{dt} (\mathcal{N} a_0^3) = 4 \pi a^2(t) \frac{da(t)}{dt},$$

we arrive at Eq. (8). The expression for the effective density of obstacles $\nu(z)$ is equal to the sum of contributions of scattering by spherical cavities [where the cross section of scattering by an individual cavity is equal to $\pi a^2(z, t, \tau)$] and scattering by randomly distributed dislocation lines. Coefficient $\pi/4$ results from averaging the cross section $\rho d \sin \theta$ of scattering by a dislocation line over all possible orientations of the line,

$$\frac{\pi}{4} \rho d = \frac{1}{4\pi} \int_0^{2\pi} d\psi \int_0^\pi d\theta \sin \theta (\rho d \sin \theta).$$

APPENDIX C

We start from Eq. (12)

$$\frac{dr}{d\Phi} = \frac{1}{r} \left(\frac{1}{Z_v + pr} - \frac{1 - \epsilon}{Z_i + pr} \right) - \frac{\epsilon}{1 + pr^2}, \quad (\text{C1})$$

where $\Phi = \phi / \pi^2 \kappa = Kt / \rho (\pi d)^2$ and $p = 4 \pi^2 \chi_0 / \kappa = 4 \pi^2 N_0 d / \rho$. This equation is equivalent to

$$\frac{dr}{d\Phi} = \frac{p[(Z_i - Z_v) - \epsilon Z_i]r^2 + \epsilon(p - Z_i Z_v)r + [(Z_i - Z_v) + \epsilon Z_v]}{r(Z_i + pr)(Z_v + pr)(1 + pr^2)}. \tag{C2}$$

It is evident that inequality $(Z_i - Z_v) - \epsilon Z_i > 0$ represents a *necessary* condition that has to be satisfied in order to obtain a solution that grows in the limit $\Phi \rightarrow \infty$. Note that if $Z_i = Z_v$ then the above condition is not satisfied. In this case any solution of Eq. (C2) corresponding to initial condition $r = 0$ at $\Phi = 0$ saturates towards $r = 1$ in the limit $\Phi \rightarrow \infty$.

Does inequality $(Z_i - Z_v) - \epsilon Z_i > 0$ represent a *sufficient* condition for the absence of saturation of growth in the limit of large doses? To answer this question we note that even if the first and the third terms in the numerator of Eq. (C2) are positive, the numerator may still have two roots situated in the vicinity of the point

$$r_0 = -\frac{\epsilon(p - Z_i Z_v)}{2p[(Z_i - Z_v) - \epsilon Z_i]}. \tag{C3}$$

The requirement that the numerator of Eq. (C2) remains non-negative at r_0 leads to inequality

$$p > Z_i Z_v + \frac{2}{\epsilon^2} [(Z_i - Z_v) + \epsilon Z_v] [(Z_i - Z_v) - \epsilon Z_i] \times \left\{ 1 - \sqrt{1 + \frac{Z_i Z_v \epsilon^2}{[(Z_i - Z_v) + \epsilon Z_v] [(Z_i - Z_v) - \epsilon Z_i]}} \right\}. \tag{C4}$$

If the latter condition, as well as inequality $(Z_i - Z_v) - \epsilon Z_i > 0$, are satisfied, then in the limit of large Φ we obtain

$$\frac{dr}{d\Phi} \sim [(Z_i - Z_v) - \epsilon Z_i] p^{-2} r^{-3}. \tag{C5}$$

The solution of the latter equation does not saturate in the limit $\Phi \rightarrow \infty$ and is given by $r(\Phi) = \sqrt{2} [(Z_i - Z_v) - \epsilon Z_i]^{1/4} \Phi^{1/4} / p^{1/2}$.

APPENDIX D

In this Appendix we describe a rigorous approach to finding solutions of Eq. (25). Consider an auxiliary equation

$$\frac{d^2 f(z)}{dz^2} - \Omega^2(z) f(z) = \text{const}. \tag{D1}$$

The corresponding *homogeneous* equation has two linearly independent solutions $f_+(z)$ and $f_-(z)$. $f_+(z)$ vanishes exponentially in the limit $z \rightarrow \infty$, and $f_-(z)$ vanishes in the limit $z \rightarrow -\infty$. Consider a function

$$F(z) = f_+(z) \int_0^z dz' f_-(z') + f_-(z) \int_z^\infty dz' f_+(z'). \tag{D2}$$

This function satisfies equation

$$\frac{d^2 F(z)}{dz^2} - \Omega^2(z) F(z) = f'_+(z) f_-(z) - f'_-(z) f_+(z). \tag{D3}$$

The linear combination of two solutions of Eq. (D1) of the form $f'_+(z) f_-(z) - f'_-(z) f_+(z)$ is their Wronskian, and is therefore a quantity that is independent of coordinate z . This shows that by choosing the normalization of $F(z)$ in a suitable way, we obtain the required solution of the inhomogeneous Eq. (D1). To satisfy the boundary condition at $z = 0$ we should add to $F(z)$ a suitable solution of the corresponding homogeneous equation. The addition of $f_+(z)$ multiplied by an appropriate numerical factor satisfies this requirement.

To find functions $f_+(z)$ and $f_-(z)$ we need to develop a numerical approach to eliminating exponentially growing terms from solutions of the homogeneous Eq. (D1). A powerful algorithm for eliminating exponentially growing solutions of systems of second-order differential equations was developed by Zhao and Tong³⁵ in the theory of reflection high-energy electron diffraction. To find a regular solution of Eq. (D1) we rewrite this equation in the form of a system of two linear equations

$$\begin{aligned} \frac{dg}{dz} &= \Omega^2(z) f(z), \\ \frac{df}{dz} &= g(z). \end{aligned} \tag{D4}$$

Assuming that $z > 0$, we consider how a solution of Eq. (D4) behaves on an (arbitrarily chosen) interval $[z_1, z_2]$, which we assume to be sufficiently small so that inside this interval function $\Omega(z)$ can be approximated by a constant $\Omega(z, t) \approx \Omega(z^*, t) = \Omega^*$, where $z^* \in [z_1, z_2]$. The matrix that relates solutions of Eq. (D4) at both ends of the interval has the form

$$\begin{pmatrix} g(z_2) \\ f(z_2) \end{pmatrix} = \begin{pmatrix} M_D(z_2 - z_1), & M_T(z_2 - z_1) \\ M_B(z_2 - z_1), & M_D(z_2 - z_1) \end{pmatrix} \begin{pmatrix} g(z_1) \\ f(z_1) \end{pmatrix}, \tag{D5}$$

where

$$\begin{aligned} M_D(z) &= \cosh(\Omega^* z), \\ M_T(z) &= \Omega^* \sinh(\Omega^* z), \\ M_B(z) &= \frac{\sinh(\Omega^* z)}{\Omega^* z}, \end{aligned} \tag{D6}$$

and $\det \hat{M} = M_D^2 - M_T M_B = 1$. Introducing the R matrix by the relation $g(z) = R(z) f(z)$, we obtain

$$R(z_1) = \frac{M_D(z_2 - z_1)R(z_2) - M_T(z_2 - z_1)}{M_D(z_2 - z_1) - M_B(z_2 - z_1)R(z_2)}. \quad (\text{D7})$$

This equation defines the rule according to which the R matrix propagates from a distant point $z \rightarrow \infty$ to the origin z

$= 0$. The entire profile of the function $f(z)$ can now be restored recurrently by using a relation similar to Eq. (D7)

$$f(z_2) = [M_D(z_2 - z_1) - M_B(z_2 - z_1)R(z_2)]^{-1} f(z_1). \quad (\text{D8})$$

-
- ¹Phase Transformations and Systems Driven Far from Equilibrium, edited by E. Ma, M. Atzmon, P. Bellon, and R. Trivedi, MRS Symposia Proceedings No. 481 (Materials Research Society, Warrendale, PA, 1998).
- ²G. Martin, Curr. Opin. Solid State Mater. Sci. **3**, 552 (1998).
- ³C.A. English and D.J. Mazey, Nuclear Energy **29**, 67 (1990).
- ⁴K. Ehrlich, Philos. Trans. R. Soc. London, Ser. A **357**, 595 (1999).
- ⁵A.D. Brailsford and R. Bullough, Philos. Trans. R. Soc. London, Ser. A **302**, 87 (1981).
- ⁶R.S. Averback and T. Diaz de la Rubia, Displacement Damage in Irradiated Metals and Semiconductors, in Solid State Physics: Advances in Research and Applications, Vol. 51, edited by H. Ehrenreich and F. Spaepen (Academic, New York, 1998), pp. 281–402.
- ⁷D.J. Bacon, F. Gao, and Y.N. Osetsky, J. Nucl. Mater. **276**, 1 (2000).
- ⁸N. Soneda and T. Diaz de la Rubia, Philos. Mag. A **78**, 995 (1998).
- ⁹C.H. Woo, B.N. Singh, and A.A. Semenov, J. Nucl. Mater. **239**, 7 (1996).
- ¹⁰D. Walgraef, in Patterns, Defects and Materials Instabilities, Vol. 183 of NATO Advanced Study Institute, Series E: Applied Sciences, edited by D. Walgraef and N. M. Ghoniem (Kluwer Academic, Amsterdam, 1990), p. 73.
- ¹¹A.A. Semenov and C.H. Woo, Appl. Phys. A: Mater. Sci. Process. **67**, 193 (1998).
- ¹²B.N. Singh, Radiat. Eff. Defects Solids **148**, 383 (1999).
- ¹³C.H. Woo, J. Comput.-Aided Mater. Des. **6**, 247 (1999).
- ¹⁴C. Sagui and M. Grant, Phys. Rev. E **59**, 4175 (1999).
- ¹⁵R. Burghaus, Phys. Rev. E **57**, 3234 (1998).
- ¹⁶Yu.N. Osetsky, D.J. Bacon, A. Serra, B.N. Singh, and S.I. Golubov, J. Nucl. Mater. **276**, 65 (2000).
- ¹⁷B.N. Singh and A.J.E. Foreman, Philos. Mag. **29**, 847 (1974).
- ¹⁸W.V. Green, S.L. Green, B.N. Singh, and T. Leffers, J. Nucl. Mater. **103/104**, 1221 (1981).
- ¹⁹A.J.E. Foreman, B.N. Singh, and A. Horsewell, Mater. Sci. Forum **15-18**, 895 (1987).
- ²⁰H. Trinkaus, B.N. Singh, and A.J.E. Foreman, J. Nucl. Mater. **206**, 200 (1993).
- ²¹H. Trinkaus, B.N. Singh, and M. Victoria, J. Nucl. Mater. **233**, 1089 (1996).
- ²²S.I. Golubov, B.N. Singh, and H. Trinkaus, J. Nucl. Mater. **276**, 78 (2000).
- ²³E. M. Lifshitz and L. P. Pitaevskii, Physical Kinetics (Pergamon, Oxford, 1981), Sec. 100, p. 432.
- ²⁴V.A. Borodin, Physica A **260**, 467 (1998).
- ²⁵J.R. Matthews, Contemp. Phys. **18**, 571 (1977).
- ²⁶A. P. Sutton and R. W. Baluffi, Interfaces in Crystalline Materials (Oxford University Press, Oxford, 1996), p. 424.
- ²⁷Handbook of Mathematical Functions, edited by M. Abramowitz and I. Stegun (Dover, New York, 1965), p. 875.
- ²⁸R. Becker and W. Döring, Ann. Phys. (Leipzig) **24**, 719 (1935).
- ²⁹Ja. B. Zeldovich, Zh. Éksp. Teor. Fiz. **12**, 525 (1942).
- ³⁰H. Vehkamäki and I. Ford, Phys. Rev. E **59**, 6483 (1999).
- ³¹M. L. Goldberger and K. M. Watson, Collision Theory (Wiley, New York, 1964).
- ³²J. M. Ziman, Models of Disorder (Cambridge University Press, Cambridge, 1979), Sec. 10.
- ³³M. Lax, Phys. Rev. **85**, 621 (1952).
- ³⁴A. Ishimaru, Wave Propagation and Scattering in Random Media (Academic, New York, 1978).
- ³⁵T.C. Zhao and S.Y. Tong, Phys. Rev. B **47**, 3923 (1993).